



Fermi National Accelerator Laboratory

CONF-960581--17

FERMILAB Conf-96/238-E
CDF

FNAL/C--96/238-E

Production and Decays of Top Quark Pairs in the Single Lepton and Dilepton Channels at CDF

M.C. Kruse
For the CDF Collaboration
*Department of Physics and Astronomy
University of Rochester
Rochester, New York 14627*

*Fermi National Accelerator Laboratory
P.O. Box 500, Batavia, Illinois 60510*

RECEIVED
SEP 23 1996
OSTI

August 1996

MASTER

Submitted to the *XIth Topical Workshop on $\bar{p}p$ Collider Physics*, Abano Terme (Padova), Italy,
May 27-June 1, 1996.

REVISIONS
BY
DATE

Disclaimer

This report was prepared as an account of work sponsored by an agency of the United States Government. Neither the United States Government nor any agency thereof, nor any of their employees, makes any warranty, express or implied, or assumes any legal liability or responsibility for the accuracy, completeness or usefulness of any information, apparatus, product or process disclosed, or represents that its use would not infringe privately owned rights. Reference herein to any specific commercial product, process or service by trade name, trademark, manufacturer or otherwise, does not necessarily constitute or imply its endorsement, recommendation or favoring by the United States Government or any agency thereof. The views and opinions of authors expressed herein do not necessarily state or reflect those of the United States Government or any agency thereof.

Distribution

Approved for public release: further dissemination unlimited.

DISCLAIMER

**Portions of this document may be illegible
in electronic image products. Images are
produced from the best available original
document.**

FERMILAB-CONF-96/238-E

CDF/DOC/TOP/CDFR/3825

August 20, 1996

**PRODUCTION AND DECAYS OF TOP QUARK PAIRS IN
THE SINGLE LEPTON AND DILEPTON CHANNELS AT CDF**

M.C. KRUSE^a

*Department of Physics and Astronomy, University of Rochester,
Rochester, New York 14627, USA*

We present the results from $t\bar{t}$ production in $p\bar{p}$ collisions at $\sqrt{s} = 1.8$ TeV, with decays into one or two leptons plus multiple jets. The full dataset accumulated by the CDF collaboration at the Fermilab Tevatron from 1992 through 1995, corresponding to a total integrated luminosity of 109.4 ± 7.2 pb⁻¹, is used.

1 Introduction

With the discovery of the top quark now more than a year old^{1,2}, focus has appropriately shifted towards a deeper understanding of the top quark properties, both in production and decay. Using the current CDF dataset, corresponding to an integrated luminosity of about 110 pb⁻¹, these properties include the top mass, the $t\bar{t}$ production cross-section, top decay branching ratios, and kinematics of the $t\bar{t}$ system. The CDF top mass measurements have been presented elsewhere in these proceedings³. The present talk will report on the cross-section and branching ratio measurements together with some top kinematics, using the $t\bar{t}$ decay channels in which at least one W boson decays leptonically to either an electron or a muon. Recent measurements using the channels in which both W 's decay hadronically, and also in which one W decays to an electron or a muon and the other to a tau, are presented in another talk of these proceedings⁴.

The dominant $t\bar{t}$ production mechanism for the conditions provided at the Tevatron collider is $q\bar{q}$ annihilation ($q\bar{q} \rightarrow t\bar{t}$), which accounts for $\sim 90\%$ of the $t\bar{t}$ pairs produced, the rest coming from gluon-gluon fusion ($gg \rightarrow t\bar{t}$). In the Standard Model the top quark decays by the charged weak current into a real W boson and a b quark with a branching fraction close to unity. The $t\bar{t}$ decays can be characterized by the W^+W^- decays. The *dilepton* category for $t\bar{t}$ decay is represented by the case in which both W bosons decay leptonically, the *lepton + jets* category by one W decaying leptonically and the other hadronically, and the *hadronic* category by both W 's decaying hadronically.

^aRepresenting the CDF collaboration, E-mail:mkruse@fnal.gov

Here we consider the *dilepton* and *lepton + jets* categories in which the lepton is an electron or a muon. Specifically, we examine;

$$\begin{aligned} \text{dilepton channel :} & \quad t\bar{t} \rightarrow \ell^+ \nu_\ell \ell^- \bar{\nu}_\ell b\bar{b} \quad (\ell = e \text{ or } \mu) \\ \text{lepton + jets channel :} & \quad t\bar{t} \rightarrow \ell \nu_\ell j j b\bar{b} \quad (\ell = e \text{ or } \mu) \end{aligned}$$

2 The CDF Detector

A detailed description of the CDF detector can be found elsewhere^{5,6}. Particle charge and momenta are measured in the central tracking chambers which reside in a 1.4 T superconducting solenoid magnet. The tracking chambers provide a pseudorapidity coverage of $|\eta| < 1.0$. Surrounding the tracking chambers, the electromagnetic and hadronic calorimeters are used in the identification and energy measurements of electrons, jets and photons. Muons are identified with drift chambers located outside the calorimeters. A three-level trigger is employed to select high transverse momentum (P_t) electrons and muons.

3 Dilepton Analysis

3.1 Event Selection

A typical $t\bar{t}$ decay in the dilepton channel will contain 2 high- P_t leptons, 2 high- E_t jets, and 2 neutrinos which provide a large missing transverse energy (\cancel{E}_t). The dilepton analysis begins by selecting events with at least 2 high- P_t ($> 20 \text{ GeV}$), oppositely charged leptons (e or μ), in the central pseudorapidity region $|\eta| < 1.0$. The lepton identification efficiencies are measured from $Z^0 \rightarrow \ell^+ \ell^-$ data events to be ~ 0.91 for muons and ~ 0.86 for electrons. At least one of the leptons is required to be isolated, in both the tracking chambers and the calorimeters, from any jet activity. We reject $Z \rightarrow \ell^+ \ell^- X$ events by requiring the dilepton invariant mass, M_{ee} or $M_{\mu\mu}$, to be outside the mass window, $75 \text{ GeV} < M_{\ell\ell} < 105 \text{ GeV}$. This cut is demonstrated in Figure 1 which shows the invariant mass distributions of the dilepton events before the invariant mass cut. The ee and $\mu\mu$ data have been separated according to jet multiplicity. Clearly the majority of dilepton events ($\sim 90\%$) before the invariant mass cut are the leptonic decays of Z bosons.

We then require the event to contain significant \cancel{E}_t , a characteristic in $t\bar{t}$ dilepton decays from the presence of neutrinos. A magnitude cut of $|\cancel{E}_t| > 25 \text{ GeV}$ is imposed, in addition to the requirement that if $|\cancel{E}_t| < 50 \text{ GeV}$ then the azimuthal angle between the \cancel{E}_t and the nearest lepton or jet, $\Delta\phi(\cancel{E}_t, \ell \text{ or } j)$, be greater than 20° . The reason for the $\Delta\phi(\cancel{E}_t, \ell \text{ or } j)$ cut is twofold. Drell-Yan

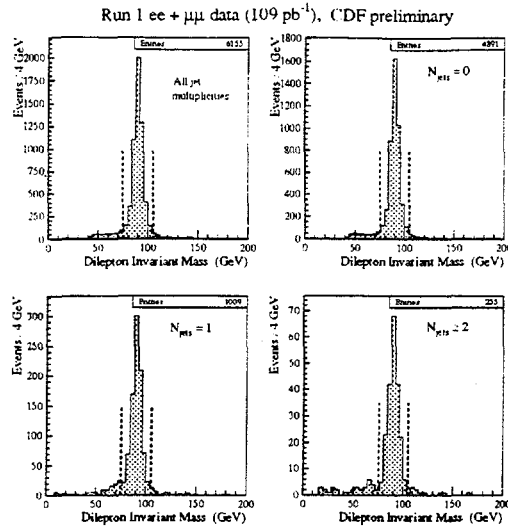


Figure 1: Dilepton (ee and $\mu\mu$) invariant mass distributions, for the different jet multiplicities, before the invariant mass cut but after lepton ID, opposite charge requirement, and isolation cuts. The dashed lines represent the invariant mass cut.

events do not contain neutrinos, so if such an event has a significant \cancel{E}_t , then it is most likely the result of a jet energy mismeasurement, thus resulting in a \cancel{E}_t direction highly correlated with the jet direction. In addition, the \cancel{E}_t direction in $Z^0 \rightarrow \tau^+\tau^-$ events tends to favor the direction of one of the leptons. The \cancel{E}_t cuts are most clearly demonstrated in Figure 2, a plot of $\Delta\phi(\cancel{E}_t, \ell \text{ or } j)$ versus \cancel{E}_t for the dilepton data in the ≥ 2 -jet bin after the isolation and invariant mass cuts. In the signal region are the 10 dilepton candidates, 1 ee , 2 $\mu\mu$ and 7 $e\mu$. The final requirement in the dilepton events is at least 2 jets with transverse energy, $E_t > 10 \text{ GeV}$, and $|\eta| < 2.0$.

3.2 Dilepton Channel Results

The number of events surviving each of the successive cuts described above are given in Table 1. There are 10 $t\bar{t}$ dilepton candidates that pass all cuts, 1 ee , 2 $\mu\mu$, and 7 $e\mu$. The expected background in the dilepton channel will be discussed below.

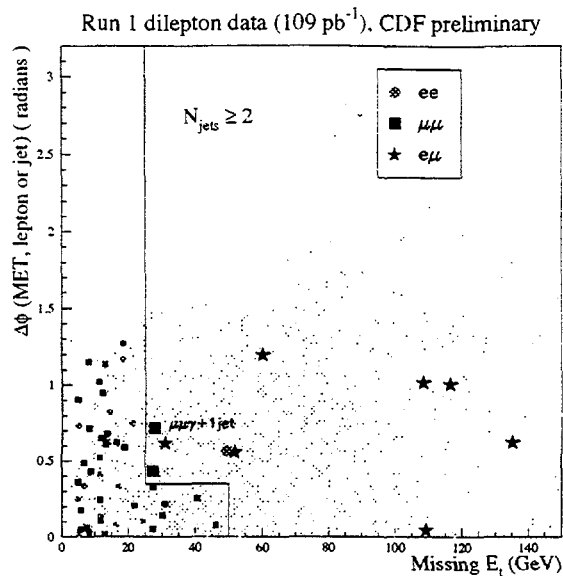


Figure 2: Azimuthal angle between the \cancel{E}_t and the nearest lepton or jet versus the \cancel{E}_t for dilepton events with at least 2 jets which have passed all except the \cancel{E}_t cuts (represented by the solid lines). The $t\bar{t}$ dilepton signal region is to the right of the \cancel{E}_t cut lines.

Table 1: CDF $t\bar{t}$ dilepton analysis results in 109 pb^{-1} for the ee , $\mu\mu$ and $e\mu$ channels. After all cuts 10 candidate events remain.

Cut	ee	$\mu\mu$	$e\mu$
lepton ID	2857	3452	68
Same-Sign	2841	3444	55
Isolation	2798	3357	49
Invariant Mass	316	375	49
Missing E_t	6	7	16
2-jet	1	2	7

3.3 Dilepton Channel Acceptance

The $t\bar{t}$ acceptance in the dilepton channel, ϵ_{dil} , is defined as the fraction of $t\bar{t}$ events expected to pass all the dilepton selection cuts described above. Note that this definition includes the dilepton branching ratio of $\frac{4}{81}$. Large statistics $t\bar{t}$ Monte Carlo samples were used to determine the acceptance. For a top mass of 175 GeV the dilepton channel acceptance is;

$$\epsilon_{dil} = (0.77 \pm 0.02(stat) \pm 0.07(syst))\%$$

The systematic error is dominated by the Monte Carlo modeling of lepton identification efficiencies (7%). The individual dilepton channels contribute to ϵ_{dil} in the following way: (15 ± 1)% ee , (27 ± 1)% $\mu\mu$, and (58 ± 2)% $e\mu$. Although, as expected, most of the dilepton acceptance is due to both W bosons decaying to either an electron or a muon (86 ± 3%), part of the acceptance is due to the case in which one W decays to a τ which subsequently decays leptonically (11 ± 1%), and also, a small fraction (3 ± 1%) arises from the lepton + jets decay mode in which the second lepton comes from the semileptonic decay of one of the b jets.

3.4 Dilepton Background

There are various sources of lepton pairs which can potentially resemble $t\bar{t}$ decay in the dilepton channel if at least 2 jets are also produced in association with the leptons. The \cancel{E}_t can come either from real neutrinos or from energy mismeasurement. The main sources of background include Drell-Yan production of lepton pairs, vector boson pair production, $Z^0 \rightarrow \tau^+\tau^-$, $W \rightarrow l\nu_l + \geq 3 jets$ with one jet faking the second lepton, and $b\bar{b}$ production.

The background contributions from the various sources are summarized in Table 2.

4 Lepton + Jets Analysis

4.1 Event Selection

A typical $t\bar{t}$ decay in the lepton + jets channel will contain 1 high- P_t lepton, 4 jets, and missing transverse energy from the neutrino. The event selection for the lepton + jets analysis requires a single, high- P_t ($> 20 GeV$), central ($|\eta| < 1.0$) lepton (e or μ), that is isolated from jet activity. In addition, there must be significant \cancel{E}_t ($\cancel{E}_t > 20 GeV$), and at least 3 energetic jets ($E_t(jets) \geq 15 GeV$) with $|\eta| < 2.0$. Here, the jet energy has been corrected for detector effects, in contrast to the dilepton analysis where just the raw jet

Table 2: Expected backgrounds in the dilepton channel after all cuts in 110 pb^{-1} . Contributions in the $ee + \mu\mu$ and $e\mu$ channels are given separately, together with the expected $t\bar{t}$ contributions (using the cross-section of reference 9 at a top mass of 175 GeV), and the CDF data results.

	Background source	Expected # of events
$e\mu$	$Z^0 \rightarrow \tau^+\tau^-$	0.38 ± 0.11
	WW	0.20 ± 0.09
	Fake leptons	0.16 ± 0.16
	$b\bar{b}$	0.02 ± 0.02
	Total Background	0.76 ± 0.21
	Expected $t\bar{t}$ ($m_{top} = 175 \text{ GeV}$)	3.5
	CDF data	7
$ee + \mu\mu$	Drell-Yan	0.62 ± 0.30
	$Z^0 \rightarrow \tau^+\tau^-$	0.21 ± 0.08
	WW	0.16 ± 0.07
	Fake leptons	0.21 ± 0.17
	$b\bar{b}$	0.03 ± 0.02
	Total Background	1.23 ± 0.36
	Expected $t\bar{t}$ ($m_{top} = 175 \text{ GeV}$)	2.4
	CDF data	3
$ee + \mu\mu + e\mu$	Others (radiative $Z^0, WZ, ZZ, Wb\bar{b}$)	0.1
	Total Background	2.1 ± 0.4
	Expected $t\bar{t}$ ($m_{top} = 175 \text{ GeV}$)	5.9
	CDF data	10

energy is used. Also, events that satisfy the dilepton analysis criteria discussed above are explicitly removed in the lepton + jets analysis.

In order to reject further the background from $W + jets$ events, we require that at least one jet be the result of b quark fragmentation. To identify such "b jets" two different techniques are employed. They are discussed in the following paragraphs. More detailed discussions can be found elsewhere⁶.

SVX tagging

The SVX tagging method uses the excellent track position resolution of the Silicon Vertex Detector (SVX) to find secondary vertices, in the transverse plane, from the tracks in jets originating from b decays. The secondary vertex is defined as the point of decay of a long-lived B meson which originated at the primary vertex. The jet is tagged if it contains a secondary vertex formed from 2 or more tracks with tight track quality cuts, or, from 3 or more tracks with looser track quality cuts. The efficiency for the SVX tagging algorithm to b -tag at least one jet in a $t\bar{t}$ decay is $(40 \pm 4)\%$.

Soft Lepton tagging

The Soft Lepton Tagging (SLT) algorithm tags jets as b jets by identifying leptons (e or μ) in the jet from the semileptonic decay of the b ($b \rightarrow c l \nu_l$) or from cascade decays ($b \rightarrow c \rightarrow s l \nu_l$). The efficiency of the SLT algorithm to detect an extra electron or muon in a $t\bar{t}$ event consistent with coming from b decay is $(20 \pm 2)\%$. About $\frac{3}{4}$ of the SLT tags in $t\bar{t}$ events are muons.

These 2 methods constitute 2 independent lepton + jets analyses, with both analyses requiring the event to contain at least 1 tagged jet by the appropriate tagging method.

4.2 Results

From the SVX tagging method 42 tags are observed in 34 events, and from the SLT tagging method 44 tags are observed in 40 events. Figures 3, 4, 5, and 6 summarize the number of observed tags as a function of jet multiplicity, both compared to the background expectations (see next section) alone, and to the background plus estimated $t\bar{t}$ contribution. In the signal region of ≥ 3 jets the data show good agreement with the expectations from background and $t\bar{t}$.

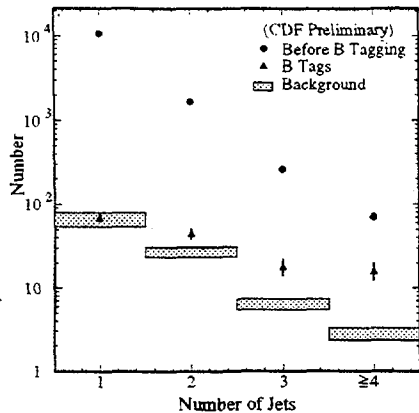


Figure 3: Jet multiplicity of events in the $t\bar{t}$ SVX analysis, compared to the estimated background.

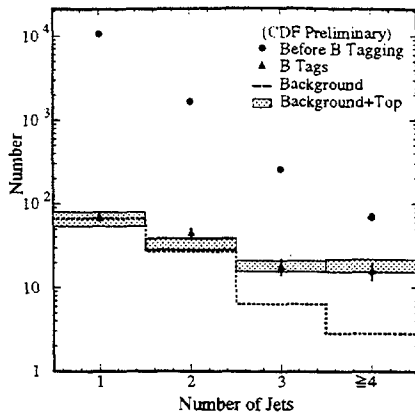


Figure 4: Jet multiplicity of events in the $t\bar{t}$ SVX analysis, compared to the estimated background + $t\bar{t}$.

Since about 70% of the 34 tagged $W + \geq 3$ jet events are expected to be from $t\bar{t}$ decay, it is worthwhile to check that the lepton and \cancel{E}_T are consistent with coming from W decay, and that the tagged jets are consistent with originating from b quarks. Figure 7 shows the W transverse mass distribution, and Figure 8 shows the $c\tau$ distribution of the SVX tagged jets. Both distributions show good agreement with what is expected from an appropriate mixture of $t\bar{t}$ and background.

4.3 Lepton + jets Background

The background in the lepton + jets analysis with SVX tagging is estimated to be 9.4 ± 1.4 events in 110 pb^{-1} , with the largest contributions resulting from $Wb\bar{b} + Wc\bar{c}$ (33%), fake tags in $W + jets$ events (25%), and $b\bar{b}$ production (23%).

For the SLT tagging analysis we have a background estimate of 25.2 ± 3.8 events, which is dominated by fake tags (92%). A summary of the background estimates for the various jet multiplicities, together with the observed numbers of tagged events, is given in Table 3.

It is noted that there is also an excess of 16 SVX tagged events in the 2 jet bin, where about 6 events from $t\bar{t}$ are expected. Observing 45 SVX tagged events in the 2 jet where 35 are expected represents a 1.5σ effect. There are several possible interpretations of this excess, which include; a statistical fluctuation, single top production, associated Higgs production (WH) with $H^0 \rightarrow b\bar{b}$ for a sufficiently low mass Higgs, or some combination of all these effects. As yet, single top production has not been included in the $t\bar{t}$ back-

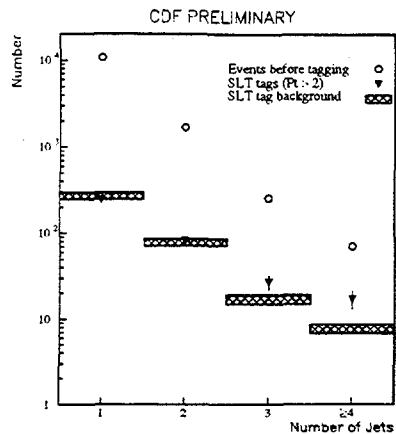


Figure 5: Jet multiplicity of events in the $t\bar{t}$ SLT analysis, compared to the estimated background.

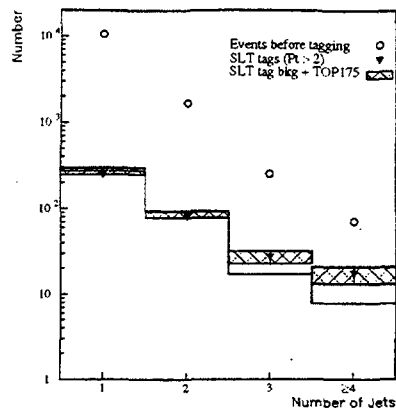


Figure 6: Jet multiplicity of events in the $t\bar{t}$ SLT analysis, compared to the estimated background + $t\bar{t}$.

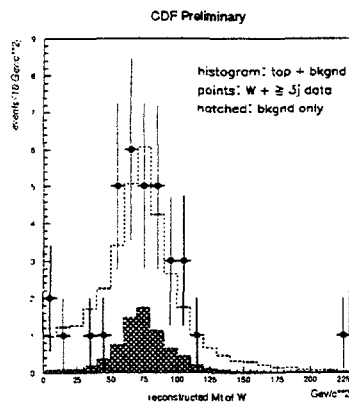


Figure 7: Transverse mass of the W in the SVX tagged $W + \geq 3$ jet events. Also shown are Monte Carlo distributions for $t\bar{t}$ + background and background alone (normalized to the background estimate).

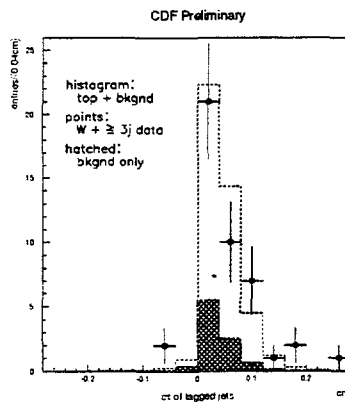


Figure 8: cr distribution of the SVX tagged jets in $W + \geq 3$ jet events. Also shown are the Monte Carlo distributions for $t\bar{t}$ + background and background alone (normalized to the background estimate).

Table 3: Expected backgrounds and data results in the lepton + jets channel after all cuts in 110pb^{-1} , for both the SVX and SLT tagging methods. The signal region is the $W + \geq 3$ jets column.

		$W + 1 \text{ jet}$	$W + 2 \text{ jets}$	$W + \geq 3 \text{ jets}$
SVX	Total Background (events)	69 ± 11	29 ± 4	9.4 ± 1.4
	# Tagged Events	70	45	34
	# Tagged Jets	70	51	42
SLT	Total Background (events)	273 ± 35	79 ± 10	25.2 ± 3.8
	# Tagged Events	245	80	40
	# Tagged Jets	245	82	44

Table 4: The $t\bar{t}$ production cross-section as measured in the dilepton and lepton + jets analyses using the CDF dataset corresponding to an integrated luminosity of $\mathcal{L} = 109.4 \pm 7.2\text{pb}^{-1}$. The acceptances are evaluated for $m_{top} = 175\text{GeV}$ and include the respective branching ratios.

Channel	Acceptance, ϵ (%)	Background, N_{bkg}	Data, N_{data}	$\sigma_{t\bar{t}}$ (pb)
DIL	0.77 ± 0.08	2.1 ± 0.4	10	$9.3^{+4.4}_{-3.4}$
SVX	3.52 ± 0.65	7.96 ± 1.37	34	$6.8^{+2.3}_{-1.8}$
SLT	1.73 ± 0.28	24.3 ± 3.5	40	$8.0^{+4.4}_{-3.6}$
Combined DIL, SVX, SLT result				$7.5^{+1.9}_{-1.6}$

ground estimate. In the signal region ~ 1.5 events are expected from the main single top production mechanisms (W^* and W -gluon fusion), with ~ 3 events expected in the 2 jet bin.

5 $t\bar{t}$ Production Cross-Section

Both the dilepton and lepton + jets analyses, discussed in the previous sections, are summarized in Table 4, and the $t\bar{t}$ production cross-section calculated for each channel ($\sigma_{t\bar{t}} = (N_{bkg} - N_{data})/\epsilon\mathcal{L}$). A better statistical measurement of $\sigma_{t\bar{t}}$ is achieved by combining all 3 channels, appropriately accounting for correlations. For a top mass of 175GeV we obtain a combined result of;

$$\sigma_{t\bar{t}} = 7.5^{+1.9}_{-1.6}\text{pb}$$

The CDF cross-section results are compared with theoretical predictions in Figure 9. Note the good agreement between individual measurements. The

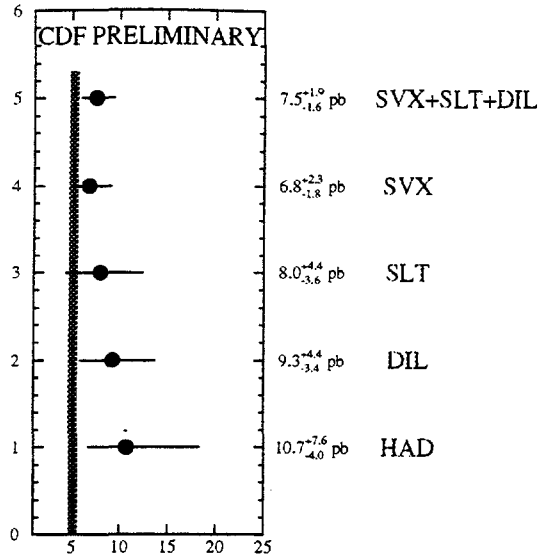


Figure 9: The CDF $t\bar{t}$ production cross-section measurements in the dilepton and lepton + jets counting experiments. Also included is the *all hadronic* measurement.

all hadronic measurement is discussed in detail in another talk ⁴. The vertical band represents the range of the central values from various theoretical calculations ^{7,8,9}.

6 $t\bar{t}$ Kinematics

The kinematic distributions of the $t\bar{t}$ system shown in this section come from a subset of the lepton + jets candidate sample, obtained with the extra requirement that there be a fourth jet in the event with $E_t > 8 \text{ GeV}$ and $|\eta| < 2.4$. This defines the so-called “mass sample” discussed in more detail in the CDF mass results ³. The kinematic distributions come from the information returned by the mass fitter used in reconstructing $t\bar{t}$ events, and are the *observed* values, meaning no attempt has been made to correct for biases from detector effects, selection cuts, or the fitting algorithm. The same is true for the Monte Carlo distributions used for comparison with the data. The sample consists of 153 events before the requirement of a b tag, with 34 of these events having at least 1 SVX or SLT tagged jet. The estimated background for the 34 tagged events is $6.4^{+2.1}_{-1.4}$ events. The background distributions in the plots have been normalized to this number.

Figures 10, 11, and 12 show the distributions in the tagged mass sample of, the invariant mass of the $t\bar{t}$ system ($M_{t\bar{t}}$), the P_t of the $t\bar{t}$ system ($P_t(t\bar{t})$), and, the P_t of the top quarks ($P_t(t)$), respectively. Such distributions provide

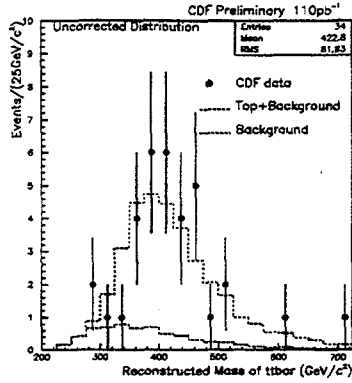


Figure 10: Reconstructed mass of the $t\bar{t}$ system in the tagged mass sample. Also shown are the Monte Carlo distributions for $t\bar{t}$ + background and background alone.

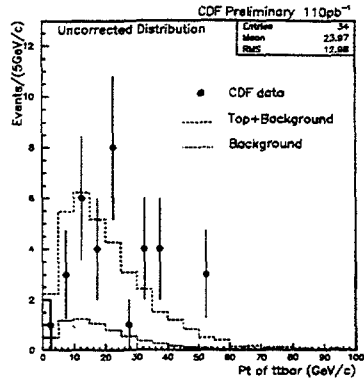


Figure 11: The transverse momentum (P_t) distribution for the $t\bar{t}$ system in the tagged mass sample. Also shown are the Monte Carlo distributions for $t\bar{t}$ + background and background alone.

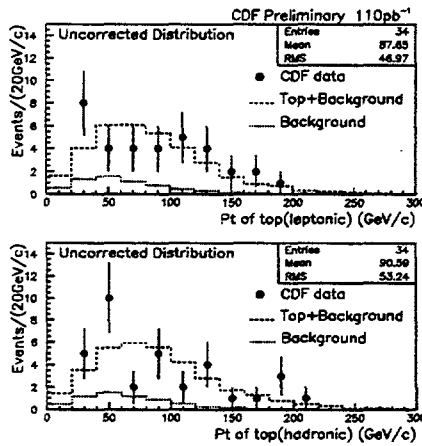


Figure 12: The P_t distributions for the top quarks in the tagged mass sample.

important checks for Standard Model predictions of $t\bar{t}$ production and decay kinematics. In particular, production of $t\bar{t}$ pairs through non-Standard Model processes may be observable in the $M_{t\bar{t}}$, $P_t(t\bar{t})$, and $P_t(t)$ distributions. Within the limited statistics of the tagged mass sample, no discrepancy with the Standard Model predictions is seen in these variables, and in others studied.

7 Direct measurement of V_{tb}

To investigate the coupling of the top quark to the bottom quark we have made the first direct measurement of the ratio of branching fractions $BF(t \rightarrow Wb)/BF(t \rightarrow Wq)$ from which we extract, by making some assumptions, the CKM matrix element V_{tb} . The following relationship exists between this ratio of branching fractions and the CKM matrix elements:

$$B \equiv \frac{BF(t \rightarrow Wb)}{BF(t \rightarrow Wq)} = \frac{|V_{tb}|^2}{|V_{td}|^2 + |V_{ts}|^2 + |V_{tb}|^2}.$$

This relationship assumes that there is no 4-th generation b' quark lighter than the top quark. If we further assume unitarity of the 3×3 CKM matrix for 3 generations, then, $|V_{td}|^2 + |V_{ts}|^2 + |V_{tb}|^2 = 1$, and so, $B = |V_{tb}|^2$. By applying the unitarity constraint and the known measurements of the other CKM matrix elements it is required that B be greater than 0.997. Thus any measurement of a smaller value of B will indicate new physics, such as a 4-th generation.

In one of two complimentary V_{tb} determinations, we used a lepton + jets sample in which the presence of a b -tagged jet was not required, but for which the $t\bar{t}$ content was enhanced by some kinematic cuts. For a pure $t\bar{t}$ sample the ratio of branching fractions, B , is simply the ratio of tagged to untagged events, divided by the tagging efficiency^b. However, the situation is more complicated for the data sample we use, mainly because of backgrounds to $t\bar{t}$ (which depend on the number of tags), and the correlation between the single and double tagging rates due to the limited geometrical acceptance of the SVX. Therefore, to account for all the extra information that goes into understanding B , we construct a likelihood function that depends on the number of events observed, and the background expected, for each bin of 0, 1 and 2 tags, together with the SVX tagging efficiency, and in which B is a free parameter. We then find the value of B which maximizes this likelihood. The same procedure is also carried out for the standard dilepton sample, and combined with the lepton +

^bOnly the SVX tagging algorithm is used here.

jets results to give the final answer. The combined result of the fit gives:

$$B = 1.25_{-0.33}^{+0.38},$$

where the errors include both statistical and systematic effects. This gives the following 95% confidence lower limits on B and V_{tb} (assuming 3 generation unitarity):

$$B > 0.61 \quad (95\% \text{ CL}),$$

$$V_{tb} > 0.78 \quad (95\% \text{ CL}).$$

A complimentary analysis which does not use an untagged sample, but which uses the standard lepton + jets sample with no extra kinematic cuts, obtains results in agreement with those above.

8 Conclusions

We have updated the single lepton and dilepton analyses for the full 110 pb^{-1} of data collected with the CDF detector. Focus has shifted from counting $t\bar{t}$ candidate events, to a deeper understanding of $t\bar{t}$ properties. Some of these properties have been reported in this talk. The combined $t\bar{t}$ production cross-section in the single lepton and dilepton channels has been measured; $\sigma_{t\bar{t}}(DIL+SVX+SLT) = 7.5_{-1.6}^{+1.9} \text{ pb}$. The first direct measurements of the CKM matrix element, V_{tb} , have been made and found to be consistent with the standard 3 generation model, though statistics are presently limited. Top properties have been explored by comparing some kinematic distributions of the $t\bar{t}$ system with Standard Model Monte Carlo. Preliminary results suggest no deviation from Standard Model predictions.

Acknowledgments

We acknowledge the exceptional performance of the Fermilab Accelerator Division, and the staffs of the participating institutions. This work was supported by the U.S. Department of Energy, the National Science Foundation, the Italian Istituto Nazionale de Fisica Nucleare, the Ministry of Education, Science and Culture of Japan, the Natural Sciences and Engineering Research Council of Canada, the National Science Council of the Republic of China, and the A.P. Sloan Foundation.

References

1. F. Abe *et al*, *Phys. Rev. Lett.* **74**, 2626 (1995).

2. F. Abachi *et al*, *Phys. Rev. Lett.* **74**, 2632 (1995).
3. Simona Rolli, Top Mass Measurement at CDF, these proceedings.
4. Sandra Leone, New Evidence for Top at CDF, these proceedings.
5. F. Abe *et al*, *Nucl. Instrum. Methods* **A271**, 387 (1988).
6. F. Abe *et al*, *Phys. Rev. D* **50**, 2966 (1994).
7. E. Laenen *et al*, *Nucl. Phys. B* **321**, 254 (1994).
8. E. Berger and H. Contopanagos, *Phys. Lett. B* **361**, 115 (1995).
9. S. Catani *et al*, CERN-TH/96-21, hep-ph/9602208 (1996).